Monte Carlo Simulation of Random Branching in Hyperbranched Polymers

E. Louise Richards,*,† D. Martin A. Buzza,‡ and Geoff R. Davies§

Department of Computing, Leeds Metropolitan University, Leeds LS6 3QS, UK; Department of Physics, University of Hull, Hull HU6 7RX, UK; and Polymers & Complex Fluids Group and Polymer IRC, School of Physics and Astronomy, University of Leeds, Leeds LS2 9JT, UK

Received January 3, 2007

ABSTRACT: We study the branching statistics of hyperbranched polymers formed from a one-pot melt polymerization of AB_2 monomers via Monte Carlo simulation. To simulate the reaction ensemble, we use a 3D percolation-type model where each lattice site of a cubic lattice is assumed to be occupied by a single AB_2 monomer and monomers are only allowed to react with their near neighbors (A reacts exclusively with B). We also allow the possibility that the reactivity ratio κ of free B groups on linear AB_2 units to those on terminal AB_2 units may be different from unity (the so-called "substitution effect"). We study the molecular weight distribution, fractal structure, loop statistics, and degree of branching as a function of both the fraction of reacted A groups p_A and the reactivity ratio κ. For $p_A \rightarrow 1$, we find that the molecular weight distribution of hyperbranched polymers with different p_A and κ collapse remarkably well on to a universal curve of the form $n(N)N_w^2 = A(N/N_w)^{-\tau} \exp(-BN/N_w)$, where $n(N)$ is the number density of HBPs with degree of polymerization N and N_w is the weight-average molecular weight (a function of p_A and κ) while A, B, and τ are constants independent of p_A and κ. Our most accurate determination of τ yields $\tau = 1.32 \pm 0.01$, which is significantly different from the mean-field value of $\tau = 1.5$. This demonstrates the importance of fluctuations in our system. The fractal dimension of HBP chains in the reaction melt is found to be in excellent agreement with the hyperscaling prediction of $d_f = 3$ [Buzza, D. M. A. *Eur. Phys. J. E* **2004**, *13*, 79] but significantly different from the mean-field result of $d_f = 4$ and the percolation result of $d_f = 2.53$. We find that the loop distribution obeys the scaling form $\hat{R}_m \propto m^{-\alpha} {p_A}^m$, where $\hat{R}_m$ is the number density of loops with degree of polymerization m and $\alpha \approx 3$ for all κ. Finally, we find excellent agreement between our simulations and the mean-field predictions for the degree of branching.

1. Introduction

Hyperbranched polymers (HBPs) are highly branched, treelike molecules formed from reactions between AB_f monomers ($f \geq 2$), where condensation occurs exclusively between the A and B groups. The product of this synthesis is a highly polydisperse mixture of randomly branched molecules. Loops may occur when a pair of reacting groups is contained within the same molecule. The properties of hyperbranched polymers have been studied since the seminal work of Flory.[1,2] There has been a resurgence of interest in these systems due to the fact that despite their random structure, they show many properties which are similar to dendrimers.[3] However, the lower cost of synthesizing hyperbranched polymers means that they are much more commercially viable compared to dendrimers. Practically, HBPs have potential applications in areas ranging from fillers for composite materials to coatings to polymer processing.

Two routes for producing HBPs that have been widely studied are the slow addition method (i.e., slow titration of AB_f monomers onto preexisting B_g cores) and the one-pot synthesis method (i.e., melt polymerization of AB_f monomers with or without B_g cores). Widmann and Davies[4] have studied the slow addition route by simulation using a method where AB_2 monomers are added sequentially onto a B_3 core. They assumed that the A group of an added monomer can react with any B group of the growing molecule, but not with a B group on itself or any other added AB_2 monomer, thus excluding the possibility of loop formation. This sequential addition model allows one to produce single molecules of well-defined molecular weight, and the structures generated using this method have been used as the starting point for a number of molecular simulation studies of HBPs.[4−6] However, the drawback of this method is that it is not able to capture the effects of polydispersity, steric hindrance, and loop formation that are inevitably present in real systems. As such, the simulation method of Widmann and Davies represents a spatially unaware mean-field model.

The one-pot route has been studied theoretically by many authors. However, with a few notable exceptions,[7−9] most studies also employ the mean-field method[1,2,10−21] where non-mean-field fluctuations are neglected. In the context of randomly branched polymers, fluctuations refer to fluctuations in the number of characteristic polymers within a characteristic volume.[22,23] When these fluctuations become large (relative to the mean value), intramolecular correlations, loops, and steric hindrance also become important. We therefore use the shorthand "fluctuations" to refer to all of these phenomena. Buzza[24] has recently shown theoretically that fluctuations are in fact relevant in 3D and cannot be neglected in HBP melts. In this paper, we study the one-pot melt polymerization of AB_2 monomers via Monte Carlo simulation of a 3D percolation-type model where each lattice site of a cubic lattice is occupied by a single AB_2 monomer and monomers are only allowed to react with their near neighbors. Since our model is spatially aware, fluctuation effects such as intramolecular correlations, loops, and steric hindrance are naturally built into our model, and our study therefore goes beyond the mean-field theory studies mentioned above. Note that our simulation scheme is "static" in the sense that chain diffusion and conformational

* Corresponding author. E-mail: L.Richards@leedsmet.ac.uk.
† Leeds Metropolitan University.
‡ University of Hull.
§ University of Leeds.

10.1021/ma0700126 CCC: $37.00
Published on Web 02/23/2007

rearrangements are not included. In essence, we are therefore assuming that the monomer reaction rate is much faster than the conformation relaxation time of the molecules. This is generally a good approximation for random branching in the melt state.[25]

As mentioned above, there have been a few theoretical studies of random branching in hyperbranched systems where fluctuation effects have also been included. Galina et al.[7] have performed a Monte Carlo simulation of a 2D percolation type model with a variable capture radius to mimic the effects of diffusion. Our simulation is therefore similar in spirit to the study of Galina et al. However, Buzza[24] has shown that in the non-mean-field regime the large-scale properties of HBPs depend critically on spatial dimension. Given that our study is performed in 3D while the study of Galina et al. was performed in 2D, our study is more directly relevant to experimental systems.

Cameron et al.[8,9] have presented a 3D Monte Carlo scheme where each monomer is mapped onto several lattice sites. By employing a bond-fluctuation model, their simulation scheme also in principle includes realistic dynamics of the starting monomers and HBP molecules. The resolution of our simulation model is lower compared to that of Cameron et al. since in our model each lattice site is occupied by a single monomer. However, while our simulation does not provide realistic information at the monomer scale, we believe that our minimal model contains enough of the essential physics to capture the large-scale properties of HBP accurately, which is in fact the primary focus of our study. Some justification for this confidence is provided by the success of the percolation model in modeling polymer gelation.[8,25] On the other hand, the advantage of adopting a minimal model (compared to higher resolution simulations) is that it enables us to simulate larger system sizes and provides us with a fast and convenient way of generating realistic starting structures for further molecular simulations.

In order to test whether our minimal model indeed captures the essential physics to model large-scale properties of HBPs, we shall compare our results with the simulations of Cameron et al. This comparison will also allow us to assess whether or not we are justified in neglecting polymer dynamics during the polymerization process. In addition, we shall also compare our simulation results with the experimental work of Kunamaneni et al.,[26,27] who reported detailed size exclusion chromatography results for a series of hyperbranched polyesters formed by cocondensation of AB monomers (57 mol %) and AB_2 monomers (43 mol %).

The rest of the paper is organized as follows. In section 2, we discuss existing theories for the molecular weight distribution, fractal dimension, loop statistics, and degree of branching for melt polymerized HBPs. In section 3, we discuss details of our Monte Carlo scheme and how we handle the data generated from our simulation. In section 4, we compare our simulation results with existing theories, the simulation results of Cameron et al., and the experimental results of Kunamaneni et al. Finally in section 5, we summarize the key conclusions of our paper.

2. Theoretical Background

As early as 1952, Flory[1,2] showed that the polycondensation of AB_f monomers leads to highly branched polymers, and he calculated the molecular weight distribution of HBPs using a statistical approach. Close to complete reaction ($p_A \rightarrow 1$, i.e., the mean-field gel point), one can show[24,25] that Flory's derivation for the number density distribution $n(N)$ (the number of hyperbranched polymers with degree of polymerization N per monomer) follows a static scaling form:

$$n(N) \cong \frac{N^{-3/2}}{N_{\mathrm{char}}^{1/2}} \exp(-N/N_{\mathrm{char}}) \tag{1}$$

where N_{char} is the characteristic largest degree of polymerization in the molecular weight distribution given by $N_{\mathrm{char}} \sim (1 - p_A)^{-2}$ in mean-field theory (p_A is the fraction of reacted A groups). The prefactor $N_{\mathrm{char}}^{1/2}$ in the equation above is a normalization constant ensuring the number density obeys the normalization condition $\int n(N)N\,\mathrm{d}N = 1$, and the symbol "$\cong$" denotes equality up to a dimensionless prefactor (of order unity).

Flory's theory is based on the assumption that there are no excluded volume interactions and no intramolecular loops and hence is a mean-field approximation. In reality, however, for short spacer lengths one cannot neglect these fluctuation effects in 3D. This has been demonstrated via computer simulation by Cameron[8] and shown theoretically by Buzza.[24] This means that for small spacer lengths mean-field theory breaks down, and eq 1 is no longer valid. Instead Buzza[24] has proposed a generalization of eq 1 for the number density in the non-mean-field regime

$$n(N) \cong \frac{N^{-\tau}}{N_{\mathrm{char}}^{2-\tau}} f(N/N_{\mathrm{char}}) \tag{2}$$

where in principle the form of the cutoff function $f(N/N_{\mathrm{char}})$ may not be exponential and the power law exponent τ may be different from the mean-field value of 3/2. In the non-mean-field regime, the simple scaling relation $N_{\mathrm{char}} \sim (1 - p_A)^{-2}$ no longer holds though obviously N_{char} is still a function of p_A. In this paper, we seek to determine τ as accurately as possible via computer simulation.[28]

A universal molar mass distribution[25] for hyperbranched polymers can be constructed by multiplying both sides of eq 2 by N_{char}^2. This gives

$$n(N)N_{\mathrm{char}}^{\ 2} \cong (N/N_{\mathrm{char}})^{-\tau} f(N/N_{\mathrm{char}}) \tag{3}$$

For hyperbranched polymers $\tau < 2$ so that $N_w \propto N_{\mathrm{char}}$ (see next paragraph). Plotting $N_w^2 n(p,N)$ vs (N/N_w) for the different extents of reaction should therefore result in the data collapsing onto universal curves. Assuming an exponential cutoff function and $N_w \propto N_{\mathrm{char}}$, eq 3 becomes

$$n(N)N_w^{\ 2} = A(N/N_w)^{-\tau} \exp(-BN/N_w) \tag{4}$$

where A and B are constants. Fitting the universal curve to eq 4 therefore provides one method for determining τ.

In terms of the number density $n(N)$, the number-average N_n, weight-average N_w, and z-average N_z degree of polymerization are defined by

$$N_n = \frac{\int n(N)N\,\mathrm{d}N}{\int n(N)\,\mathrm{d}N} \tag{5}$$

$$N_w = \frac{\int n(N)N^2\,\mathrm{d}N}{\int n(N)N\,\mathrm{d}N} \tag{6}$$

$$N_z = \frac{\int n(N) N^3 \, dN}{\int n(N) N^2 \, dN} \tag{7}$$

Inserting eq 2 into eqs 5−7, we find for hyperbranched polymers ($\tau < 2$) that $N_n \sim N_{char}^{2-\tau}$, $N_w \sim N_{char}$, and $N_z \sim N_{char}$ for $N_{char} \gg 1$. This means that

$$N_w \propto N_n^{1/(2-\tau)} \tag{8}$$

Therefore, plotting N_w vs N_n provides an alternative method for finding τ.

The fractal dimension, d_f, is defined in terms of the degree of polymerization N and the radius of gyration R_g via the relation $N \sim R_g^{d_f}$. In systems belonging to the percolation universality class (e.g., polymer gels within the Ginzburg zone), $\tau > 2$ and the fractal dimension d_f is related to the exponent τ and the dimensions of space d via the hyperscaling relation[25,29,30] $d_f = d/(\tau - 1)$ for $1 \le d \le 6$. A similar analysis for the hyperbranched polymers using the Ginzburg approach (see Buzza[24]) shows that hyperbranched polymers do not belong to the percolation universality class. This leads to hyperbranched polymers obeying a modified hyperscaling relation within the Ginzburg zone given by

$$d_f = d, \quad \text{for } d \le 4 \tag{9}$$

i.e., d_f is independent of τ.

As mentioned earlier, loop formation is important in HBP systems. For linear chains formed by the melt polymerization of linear AB monomers, Jacobson and Stockmayer[31] found that the number density of loops $\hat{R}_m$ (number of loops with degree of polymerization, m, divided by the number of monomers in the system) obeyed the scaling form

$$\hat{R}_m \propto m^{-\alpha} {p_A}^m \tag{10}$$

where p_A is the fraction of A groups that have reacted and $\alpha = 5/2$. Although eq 10 was derived for linear chains, we shall use it to analyze loop statistics in our HBP systems by allowing α to be a fitting parameter that characterizes the loop distribution.

An important parameter used to characterize the structure of HBPs is the degree of branching (DB), which is defined as[10]

$$\mathrm{DB} = \frac{2D}{2D + L} \tag{11}$$

where D is the fraction of dendritic AB_2 monomers (i.e., where both B groups have reacted) and L is the fraction of linear AB_2 monomers (i.e., where only one B group is reacted). AB_2 monomers where both B groups are unreacted are known as terminal units, denoted T. Widmann and Davies[4] have cautioned against over interpreting DB since it does not provide an unequivocal measure of the large-scale topology of HBPs. Notwithstanding this fact, DB is of considerable interest experimentally because it can be measured directly via NMR and therefore provides an additional point of contact between theory and experiment. In this paper, we shall compare our simulation results of DB with the mean-field calculations of Holter and Frey.[14]

3. Monte Carlo Simulation and Data Analysis

3.1. Simulation Details. The model assumes that each site in a 3D cubic lattice with box size L is occupied by a single AB_2 monomer. An A group is selected at random, and an attempt is made to form a bond between this A group and a randomly selected B group on this monomer or at any of its 26 near neighbors, i.e., all the monomers in a cube of length $2 \times 2 \times 2$ units centered on the first monomer that was selected. We initially considered six nearest neighbors only but found that the molecules produced were far too small compared with what is seen in experiments.[26,27] The selection of B group is regardless of whether that B group has already reacted. If the selected B group has already reacted, then we discard the A and B group pair selected and choose a new A, B pair using the procedure described above. If the selected B group is unreacted, a chemical bond is formed between the selected A, B pair. This protocol ensured unbiased statistics in our MC simulation.

The fact that we allow reactions between A and B groups on the same monomer means that we allow intramonomer loops. In effect, this means that we assume that the A and B groups on the same monomer are connected by flexible spacers. This assumption is similar to that used in the work of Cameron et al.[8,9] and Galina et al.[18,21] It is also consistent with the experimental system of Kunamaneni et al.[26,27] where the 53 mol % of AB monomers effectively acts as spacers. We found that the assumption of intramonomer loops was necessary to reproduce the polydispersity exponents τ found in the experiments of Kunamaneni et al.[26,27] (see section 4).

We assume periodic boundary conditions for the 3D cubic lattice; i.e., the nearest neighbors of monomers lying on the faces of the 3D lattice are assumed to be the monomers on the opposite faces. This eliminates the need for consideration of otherwise troublesome boundary monomers. A simulation box size of $L = 100$ was used to obtain all the results in section 4. In section 3.3, we show that this value of L is larger than the size of the largest characteristic HBPs, thus ensuring that our simulations are free from finite size effects. For $L = 100$ and $p_A \to 1$, we typically have of the order of 10^4 molecules within the simulation box, ensuring that we have good statistics for the molar mass distribution.

In order to vary the topology of the HBPs formed, we vary the local "chemistry" by assigning a variable reaction probability to the unreacted B groups. We use the notation of Widmann and Davies[4] and define the ratio of reaction probabilities, κ, as $\kappa = P_2/P_1$. Here P_1 is the reaction probability of an unreacted B group whose neighboring B group on the same monomer unit is also unreacted (i.e., a terminal AB_2 unit), and P_2 is the reaction probability of an unreacted B group whose neighboring B group on the same monomer unit is already reacted (i.e., a linear AB_2 unit). Values of $\kappa \neq 1$ correspond to the so-called "substitution" effect seen in many chemical systems. We consider three cases: $\kappa = 1$, $\kappa = 3$ (which leads to a higher degree of branching), and $\kappa = 1/3$ (which leads to a lower degree of branching). For $\kappa = 1$, we use the simulation procedure described at the beginning of this section. For $\kappa = 3$, a bond is formed if the selected (unreacted) B group belongs to a terminal unit, while a bond is formed with a 1 in 3 probability if the B group belongs to a linear unit. For $\kappa = 1/3$, a bond is formed if the selected (unreacted) B group belongs to a linear unit, while a bond is formed with a 1 in 3 probability if the B group belongs to a terminal unit. Since we are primarily interested in the large-scale behavior of HBPs, we focus on the regime where the fraction of reacted A groups p_A is close to unity; this is the regime where large molecules are formed. Specifically, all the results reported in section 4 are for $p_A = 0.96$, 0.97, 0.98, 0.99, and 1.

In order to estimate the error in the quantities calculated from the simulation data, we run each simulation three times, seeding the random number generator differently each time. The quantities and errors quoted in section 4 are the mean and standard deviation of the three sets of data thus obtained.

3.2. Number Density, *n*(*N*), and Average Molecular Weight. We characterize the molecular weight distribution of the ensemble via the number density distribution $n(N)$. In fact, for practical calculations, it is more convenient to use the logarithmic number density distribution $n(\log N)$. Specifically $n(N)\,\mathrm{d}N$ and $n(\log N)\,\mathrm{d}N$ are the number of molecules with degree of polymerization N in the interval $N \rightarrow N + \mathrm{d}N$ and $\log N \rightarrow \log N + \mathrm{d}\log N$, respectively, divided by the total number of monomers in the system. For a physical slice of the molar mass distribution, the number of molecules is the same regardless of the distribution function we use, hence

$$n(N)\,\mathrm{d}N = n(\log N)\,\mathrm{d}\log N \Rightarrow n(N) = n(\log N)/N \tag{12}$$

where we have used $\mathrm{d}(\log N) = \mathrm{d}N/N$ to derive the second equality. From the definitions of $n(N)$, $n(\log N)$ we have the normalization conditions

$$\int n(N)N\,\mathrm{d}N = \int n(\log N)N\,\mathrm{d}(\log N) = 1$$

The quantity $n(\log N)$ (and hence $n(N)$) is calculated in practice as follows. To analyze data that ranges in molecular weight from one to many hundreds, the data are binned logarithmically, i.e., in bin sizes, 1, 2−3, 4−7, 8−15, 16−31, etc. The advantage of binning the data in logarithmic bins rather than in linear bins is that the full range of molecular weights can be analyzed and plotted, rather than a restricted range as in Cameron et al.[8,9] We use N_i to represent the average molecular weight of the ith bin, where N_i is the geometric mean of the molecular weights at the bin boundaries, i.e., $N_i = \sqrt{(\text{upper bin boundary} \times \text{lower bin boundary})}$. We denote the number of molecules in the ith logarithmic bin as $\eta(\log N_i)$. The first three bins, containing only very small molecules and unreacted monomers, are discarded when analyzing the number density distribution but are included in all calculations of the number-, weight-, and z-average degree of polymerization of the system. In order to relate $n(\log N)$ to $\eta(\log N)$, we note that $n(\log N)$ is proportional to $\eta(\log N)$, i.e. $n(\log N) = A\eta(\log N)$. From the normalization condition for $n(\log N)$, we then find that $A = 1/\sum\eta(\log N_i)N_i$, where the summation is carried out over logarithmic bins. Therefore

$$n(\log N_i) = \frac{\eta(\log N_i)}{\sum\eta(\log N_i)N_i} \tag{13}$$

and

$$n(N_i) = \frac{\eta(\log N_i)}{N_i\sum\eta(\log N_i)N_i} \tag{14}$$

where we have used eq 12 to derive eq 14. The number-, weight-, and z-average degree of polymerization of the system are defined in terms of $\eta(\log N_i)$ by the discrete versions of eqs 5−7:

$$N_\mathrm{n} = \frac{\sum\eta(\log N_i)N_i}{\sum\eta(\log N_i)} \tag{15}$$

$$N_\mathrm{w} = \frac{\sum\eta(\log N_i)N_i^2}{\sum\eta(\log N_i)N_i} \tag{16}$$

$$N_z = \frac{\sum\eta(\log N_i)N_i^3}{\sum\eta(\log N_i)N_i^2} \tag{17}$$

where all the summations above are carried out over the logarithmic bins.

3.3. Radius of Gyration. For each molecule in the ensemble, we also calculate the radius of gyration, R_g, given by

$$R_\mathrm{g}^2 = \frac{1}{2}\frac{1}{N^2}\sum_{i=1}^{N}\sum_{j=1}^{N}(\mathbf{R}_i - \mathbf{R}_j)^2 \tag{18}$$

where N is the number of monomers in the molecule and $\mathbf{R}_i$ and $\mathbf{R}_j$ are the vector positions of the ith and jth monomers, respectively. Since the data are binned logarithmically, depending on the molecular weight of the molecules, a value which represents the radius of gyration for any given bin must be used. For the ith bin, we use the z-average radius of gyration of all molecules in the ith bin, which is given by

$$R_{\mathrm{g}i}^2 = \frac{\sum_\alpha N_\alpha^2 R_{\mathrm{g}\alpha}^2}{\sum_\alpha N_\alpha^2} \tag{19}$$

where the sum is over all the molecules α in the ith bin, N_α is the degree of polymerization of molecule α, and $R_{\mathrm{g}\alpha}^2$ is the radius of gyration squared for molecule α. Finally, the effective correlation length of the system is given by the z-averaged R_g^2 for the entire sample,[29] i.e.

$$R_{\mathrm{g}z}^2 = \frac{\sum_i \eta(\log N_i)N_i^2 R_{\mathrm{g}i}^2}{\sum_i \eta(\log N_i)N_i^2} \tag{20}$$

In order to determine the fractal dimension, we perform a log−log plot of $R_{\mathrm{g}i}$ vs N_i and $R_{\mathrm{g}z}$ vs N_w and N_z. The value for the fractal dimension, d_f, can then be determined from the slope of these plots, since

$$R_{\mathrm{g}i} \sim N_i^{1/d_\mathrm{f}} \tag{21}$$

and

$$R_{\mathrm{g}z} \sim N_\mathrm{char}^{1/d_\mathrm{f}} \sim N_\mathrm{w}^{1/d_\mathrm{f}} \sim N_z^{1/d_\mathrm{f}} \tag{22}$$

where we have used the fact that $N_\mathrm{char} \sim N_\mathrm{w} \sim N_z$ (for $N_\mathrm{char} \gg 1$) to obtain the second and third scaling expressions in eq 22.

In order to check the influence of box size on our simulation, we carried out our simulations on box sizes $L = 50$ and $L = 100$ and found that the calculated values such as τ and d_f agreed with each other to within 1 decimal place. This result is consistent with the fact that for all our simulations we find that the system correlation length $R_{\mathrm{g}z}$ is much smaller than the simulation box size L (e.g., for $\kappa = 1$, $p_\mathrm{A} = 1$, we find $R_{\mathrm{g}z} = 6.0$ for $L = 100$ and $L = 50$). This means that finite size effects are not important, and we are effectively simulating a bulk (i.e., infinite) HBP system. In section 4, we only present the $L = 100$ data.

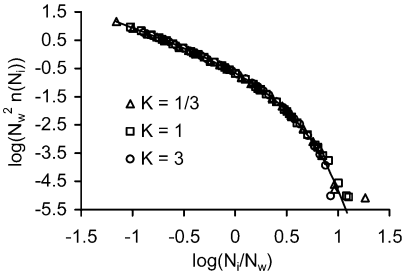

Figure 1. Universal curve for reaction ratio $\kappa = 1, {}^1/_3$, and 3.

3.4. Loop Analysis and Degree of Branching. We have calculated the fraction of looped molecules as a function of the reaction extent, p_A. We also analyze the distribution of loop sizes. Since the loop sizes generated by the Monte Carlo simulation are generally small, we bin loop sizes linearly (rather than using logarithmic bins as before) and calculate the number density of loops (number of loops with degree of polymerization m divided by the number of monomers in the system) $\hat{R}_m$. Finally, we have calculated the degree of branching DB as defined by eq 11 for different values of p_A and κ.

4. Results

4.1. Molar Mass Distribution. In Figure 1 we plot $N_w^2 n(N)$ vs (N/N_w) for the different extents of reaction p_A and for the three different values of κ: $\kappa = 1, {}^1/_3$, and 3. We see that the data collapse remarkably well onto a universal curve, indicating that the scaling assumption given by eq 1 is obeyed to a very good approximation and that the number density is universal with respect to variations in p_A and κ. In Figure 1 we also show a fit to the simulation data using eq 4, i.e., assuming the cutoff function to be an exponential and using A, B, and τ as fitting parameters. Note that the data points from high molecular weight bins are very noisy as there are only a few molecules in these bins. In order to reduce the impact of these data points on the fitting, we weighted each data point according to the number of molecules in that bin when performing the least-squares fit. This procedure yielded the fitting parameters $\tau = 1.32 \pm 0.01$ and $B = 0.72 \pm 0.01$, and the resultant fit is shown in Figure 1. We note that the fit to the data is excellent, indicating that the exponential cutoff function is a good approximation to the actual cutoff function.

In order to check for any systematic variations in the fitted values due to variations in κ, we also fitted the data for different κ separately using the same procedure as for the composite data set (for each κ, we construct a universal curve from data for different p_A). The results are collected in Table 1 (row denoted "universal curve"). We note that the τ values obtained for the different κ agree with each other within error, thus confirming that to a very good approximation the number density for our HBP system is universal with respect to variations in κ.

It is well-known that obtaining exponents from Monte Carlo data can be a rather delicate matter.[29] In order to check that the value of τ we have obtained above is a faithful reflection of the data and not an artifact of using too many fitting parameters, we have also performed a two-parameter fit of the data in Figure 1 using eq 4, assuming $\tau = 1.5$ and using A and B only as our fitting parameters. The results of this two-parameter fit and the original three-parameter fit are shown in Figure 2, where we highlight the power law regime of the log−log plot since differences in τ show up most clearly in this region. Clearly, the two-parameter fit produces a much poorer fit to the data compared to the three-parameter fit. This proves that the exponent cannot have the mean-field value of $\tau = 1.5$, and instead the three-parameter fit provides a more accurate value for τ.

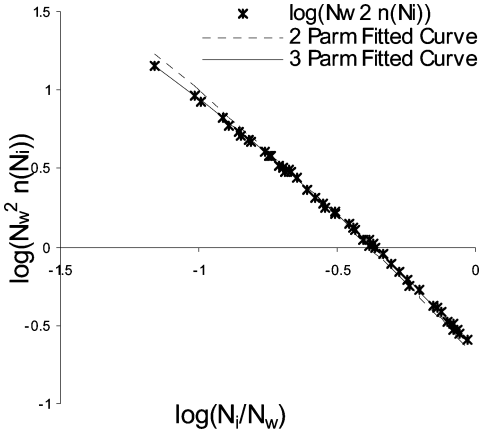

Figure 2. Two- and three-parameter fits of linear region.

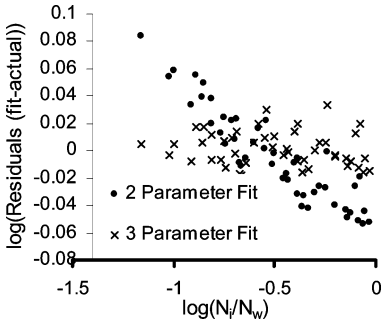

Figure 3. Residuals (fit-actual) vs N_i/N_w.

To further analyze the validity of the three-parameter fit over the two-parameter fit, in Figure 3 we log−log plot the residuals (fitted data − simulation data) vs N_i/N_w. The graph clearly shows a systematic variation in the two-parameter fit compared with a random variation in the three-parameter fit, which provides evidence that the three-parameter fit is a more valid method for fitting the simulation data.

As a final proof that the three-parameter fit allows us to determine τ accurately, we have studied simulation results obtained from a mean-field percolation model (i.e., where A and B groups are allowed to react with equal probability regardless of spatial distance between them).[32] Using the three-parameter fitting protocol outlined at the beginning of this section, we obtain for this system $\tau = 1.46 \pm 0.05$, which within error agrees with the known theoretical value of $\tau = 1.5$.

We note that the value of 1.32 ± 0.01 derived from fitting to the universal curve is different from the experimental data of Suneel et al.,[26] who found $\tau = 1.53 \pm 0.05$, and the simulation data of Cameron et al.,[8] who found $\tau = 1.488 \pm$

Table 1. Tabulated Results for Calculated Values of τ

	composite $\kappa = 1, {}^1/_3, 3$	$\kappa = 1$	$\kappa = {}^1/_3$ (more linear)	$\kappa = 3$ (more branched)
universal curve	1.32 ± 0.01	1.27 ± 0.04	1.45 ± 0.11	1.25 ± 0.05
universal curve ($N_i/N_w < 0.3$)	1.45 ± 0.01	1.42 ± 0.04	1.50 ± 0.09	1.44 ± 0.03
$n(N_i)$ vs N_i for $p_A = 1$ (linear binning)		1.50 ± 0.03	1.50 ± 0.02	1.58 ± 0.03
N_w vs N_n		1.47 ± 0.03	1.63 ± 0.01	1.28 ± 0.03

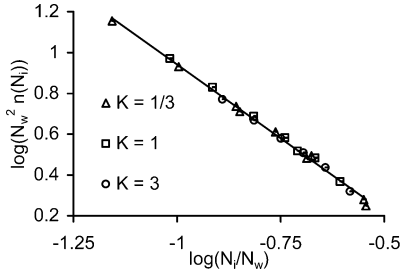

Figure 4. Straight line fit to universal curve where $N_i/N_w < 0.3$, reaction ratio $\kappa = 1$, $^1/_3$, 3, and $\tau = 1.45 \pm 0.01$.

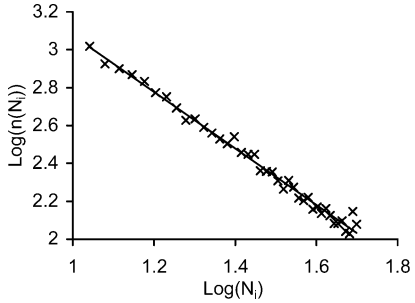

Figure 5. Linear binning of molar mass distribution, $N_i < 50$, $\kappa = 1$.

0.006. However, our analysis method is different from Suneel et al.,[26] who plotted the approximately linear region at the low molar mass end of the universal scaling plot, i.e., where $N_i/N_w < 0.3$, and Cameron et al.,[8] who log−log plot the first 50 molecular weight bins, binned linearly. To check whether our results are consistent with these methods, we replicate their analyses on our simulation data.

In Figure 4, we replicate the analysis of Suneel et al.[26] and plot the approximately linear region at the low molar mass end of the universal scaling plot, i.e., where $N_i/N_w < 0.3$. This gives a value of $\tau = 1.45 \pm 0.01$, in close agreement with Suneel et al.,[26] who found $\tau = 1.53 \pm 0.05$. Note that if we do not allow intramonomer loops, essentially all monomers become incorporated into larger molecules as we approach complete reaction of the A groups. This causes the monomer concentration to be depressed relative to the higher molecular weight species and leads to a much lower value of $\tau = 1.26 \pm 0.01$. We conclude from this fact that allowing intramonomer loops is closer to the experimental systems we are trying to model.

In Figure 5, we plot the molar mass distribution binned linearly as in Cameron et al.[8] rather than logarithmically. We note that at the extent of reaction of 100%; i.e., when all A groups have reacted and each molecule contains one cycle, we calculate a value of 1.50 ± 0.03 for $\kappa = 1$, by straight line fitting through the data. This is in close agreement with Cameron et al.,[8] who found $\tau = 1.488 \pm 0.006$.

However, we argue that the analyses used by Suneel et al.[26] and Cameron et al.[8] are inaccurate because the slope of their plots is affected by cutoff effects, hence yielding an incorrect value for τ. This can be shown as follows. Assuming an exponential cutoff, the universal fit function is given by eq 4. Taking log (base 10) of both sides of eq 4, we find

$$\log n(N)N_w^2 = \log A - \tau \log \frac{N}{N_w} - B\frac{N}{N_w}\log e$$

Writing $y = \log n(N)N_w^2$ and $x = \log(N/N_w)$, we have

$$y = \log A - \tau x - B10^x \log e$$

For low molecular weights where $x \ll 1$, the apparent value of τ obtained by fitting the linear region is therefore given by

$$\tau_{app} = -\frac{dy}{dx} = \tau + B10^x(\log e)^2 \approx \tau + B(\log e)^2 \quad (23)$$

Testing eq 23 with the universal curve data for $-1.5 < \log(N_i/N_w) < -0.6$, we find a value of $\tau_{app} = 1.45 \pm 0.01$ from a straight line fit (unweighted) to the data while the calculated value of τ_{app} from eq 23 using the fitted parameters of the universal curve ($B = 0.72$, $\tau = 1.32$) is 1.46. The excellent agreement between the two values thus confirms that eq 23 is accurate and there is a nonnegligible contribution from the cutoff function to the slope of the linear region of the data.

Note that from eq 23 the correction to τ due to the cutoff function is always present on a log−log plot *no matter how small we go in molecular weight*. In particular, the correction is present even for systems with $N_{char} \gg 1$ where there exists a well-defined linear region of data far from the cutoff function. Therefore, when trying to determine τ from the universal plot, we must always include the cutoff function in our fitting. In this context, it is important to emphasize the exponential cutoff function that we have assumed gives good fits to the universal data in Figure 1 and should therefore be a good approximation to the true cutoff function for our system. This in turn means that the values of τ that we have determined from direct fitting to the universal curves should be a good approximation to the true value of τ. An additional benefit of using an exponential cutoff function is that, since this is the same form predicted by mean-field theory, we can isolate the effect of fluctuations to a single parameter τ. Specifically, we can quantify the strength of these fluctuations by looking at how far τ deviates from the mean-field value of $\tau = 1.5$.

Notwithstanding the fact that the τ values obtained by Suneel et al.[26] and Cameron et al.[8] are probably inaccurate because of the neglect of the cutoff function, the good agreement between our results and those of these authors (when the data are subject to the same method of analysis) suggests that our minimal model captures the essential physics and microscopic details of these more complex systems. This gives us confidence that our simple percolation-type model is capable of producing experimentally relevant HBP ensembles. The good agreement also provides a post hoc justification for using a static percolation model (i.e., where we neglect chain relaxations) to simulate the one-pot melt polymerization of HBPs. Evidently, the experimentally relevant regime for this system is the so-called equilibrium gelation regime rather than the kinetic gelation regime.[25]

For the sake of completeness, we have also analyzed data for different κ using the method of Suneel et al.[26] and Cameron et al.,[8] and we find very weak dependencies of the fitted τ values on κ (see Table 1). This confirms our earlier conclusion that the number densities are to a very good approximation universal with respect to variations in κ.

An alternative method for determining τ that does not require prior knowledge of the cutoff function relies on analyzing the scaling of N_w against N_n (see eq 8). A similar method has been used successfully to determine τ for gelation ensembles (in that case one analyzes the scaling of N_{char} against N_w).[33,34] In Figure 6, we plot N_w vs N_n for $\kappa = 1$. From the slope of the log−log plot, we find 1.47 ± 0.03. We have also repeated this calculation for other values of κ, and the results are summarized in Table 1.

We note that the value $\tau = 1.47 \pm 0.03$ determined from the scaling of N_w vs N_n for $\kappa = 1$ is significantly different from the value $\tau = 1.32 \pm 0.01$ determined earlier from fitting the universal curve. However, from Table 1, we also note that there

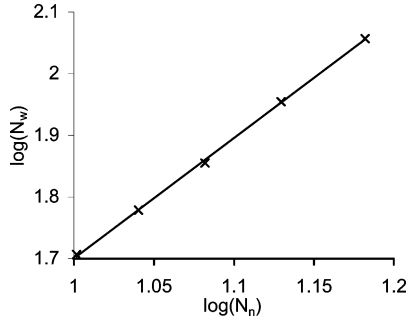

Figure 6. Plot of $\log(N_w)$ vs $\log(N_n)$, reaction ratio $\kappa = 1$.

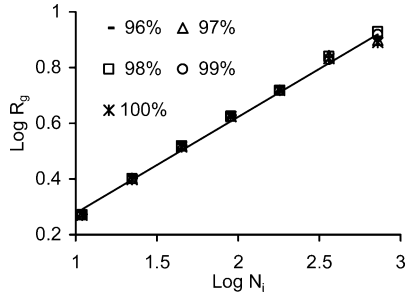

Figure 7. $d_f = 2.87 \pm 0.08$ from 1/slope of $\log(R_{gi})$ vs $\log(N_i)$, reaction ratio $\kappa = 1$.

is a large variation of τ with κ for τ determined from the scaling of N_w vs N_n. This is clearly inconsistent with Figure 1, and the other methods of analysis in Table 1 which all show that τ is essentially universal with respect to variations in κ. We believe that the discrepancy arises from the fact that eq 8 is only strictly valid in the limit $N_{char} \gg 1$. Since N_{char} is not very large for our HBPs, the sensitivity of N_n (and to a much lesser extent N_w) to the lower cutoff mass introduces large systematic errors to the determination of τ via the scaling of N_w vs N_n. Because of the above problem, we believe that direct fitting of the universal curve with an assumed form for the cutoff function represents the most accurate means for determining τ for HBP systems. In contrast to HBPs, much higher values for N_{char} are achievable for gelation systems. In addition, both N_w and N_{char} are much less sensitive to the lower cutoff mass compared to N_n (see eqs 15−17). The corresponding scaling relation between N_{char} vs N_w therefore serves as a much more accurate means for determining τ for gelation systems.

To summarize, assuming an exponential cutoff function, our best estimate for τ (determined from universal plots) is 1.32 ± 0.01. This is significantly different from the mean-field value of $\tau = 1.5$, and we attribute the difference to the importance of fluctuations (e.g., loops and excluded volume effects) in our system. A similar effect is observed for percolation clusters[25,29] where mean-field theory predicts $\tau = 2.5$, but the observed value for critical percolation is $\tau = 2.18$.

4.2. Radius of Gyration. In Figure 7 we plot R_{gi}, the average radius of gyration of all molecules in the ith bin, vs N_i, the bin average degree of polymerization, for $\kappa = 1$. The fractal dimension d_f can be determined from the slope of the log−log plot (eq 21) from which we find $d_f = 2.87 \pm 0.08$. The fractal dimension for $\kappa = {}^1/_3$ and $\kappa = 3$ are determined similarly, and we find $d_f = 2.84 \pm 0.06$ and $d_f = 2.84 \pm 0.09$ for $\kappa = {}^1/_3$ and $\kappa = 3$, respectively. We note that all these values for d_f are very consistent with each other and close to the value $d_f = 3$ predicted by eq 9.

Another method for determining d_f is via the scaling of R_{gz}^2 vs N_{char} (eq 22). Recall that in the limit $N_{char} \gg 1$ $N_{char} \sim N_w$, N_z. Therefore, in Figure 8 we plot R_{gz}^2 vs N_w while in Figure 9

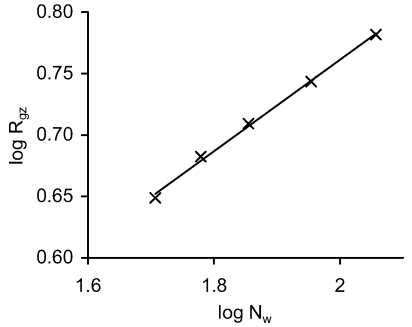

Figure 8. $d_f = 2.80 \pm 0.26$ from 1/slope of $\log(R_{gz})$ vs $\log(N_w)$, reaction ratio $\kappa = 1$.

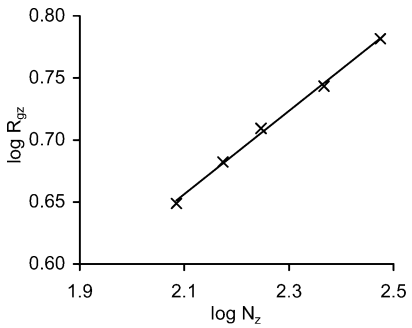

Figure 9. $d_f = 3.00 \pm 0.08$ from 1/slope of $\log(R_{gz})$ vs $\log(N_z)$, reaction ratio $\kappa = 1$.

Table 2. Tabulated Results for Calculated Values of d_f

box size, $L = 100$	$\kappa = 1$	$\kappa = {}^1/_3$ (more linear)	$\kappa = 3$ (more branched)
R_{gi} vs N_i	2.87 ± 0.08	2.84 ± 0.06	2.84 ± 0.09
R_{gz} vs N_w	2.80 ± 0.26	2.84 ± 0.19	2.84 ± 0.02
R_{gz} vs N_z	3.00 ± 0.08	3.03 ± 0.06	2.92 ± 0.28

we plot R_{gz}^2 vs N_z for $\kappa = 1$. From the slope of the log−log plot, we find $d_f = 2.80 \pm 0.26$ and $d_f = 3.00 \pm 0.08$ from Figures 8 and 9, respectively. The corresponding results for $\kappa = {}^1/_3$ and $\kappa = 3$ are also collected in Table 2.

We note that the d_f results for different κ from the scaling of R_{gz}^2 vs N_w and N_z are in very good agreement with each other and close to the value $d_f = 3$ predicted by eq 9 (indeed, most of these results are the same as $d_f = 3$ within error). In summary, the results for d_f obtained from the scaling of R_{gi} vs N_i and R_{gz} vs N_w, N_z are within error either the same as or very close to the hyperscaling prediction $d_f = 3$ (eq 9). Our results are significantly different from the mean-field prediction of $d_f = 4$, which once again points to the importance of fluctuations in our system.

Finally, we note that our simulation results for d_f and τ are significantly different from those of percolation theory. Specifically from our simulations, we find $d_f \approx 3$ and $\tau = 1.32 \pm 0.01$ (or alternatively $\tau_F = 2$ (see ref 28)) while the corresponding results for percolation theory are $d_f = 2.53$ and $\tau = 2.18$.[25,29] In an earlier paper[24] we also showed that the upper critical dimension for HBPs is $d_u = 4$ compared to $d_u = 6$ for percolation clusters. These results show that HBPs do not belong to the same universality class as critical percolation even at or very close to the mean-field gel point (i.e., $p_A = 1$).

4.3. Loop Statistics and Degree of Branching. In Figure 10 we plot the fraction of loops vs reaction extent. We see that full cyclization occurs for $p_A = 1$, consistent with the results of Cameron et al.[8,9] The results in Figure 10 provide direct confirmation that looping is important in our system.

In Figure 11 we plot $\hat{R}_m/{p_A}^m$ vs m for $\kappa = 1$, where $\hat{R}_m$ is the number density of loops with degree of polymerization m. The

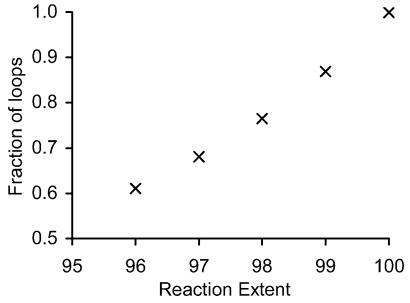

Figure 10. Fraction of loops vs reaction extent p_A, reaction ratio $\kappa = 1$.

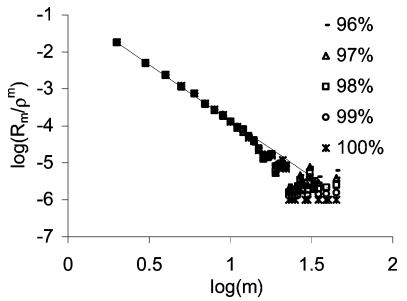

Figure 11. Number density of loops $\hat{R}_m$ vs m, loop size, reaction ratio $\kappa = 1$.

Table 3. DB from Our Simulations Compared to Mean-Field Predictions of Holter and Frey[14] (Reported to 3 Significant Figures)

	our simulation	Holter and Frey[14]
$\kappa = 1$, $p_A = 0.96$	0.4741 ± 0.0002	0.480
$\kappa = 1$, $p_A = 1.00$	0.4952 ± 0.0001	0.500
$\kappa = 1/3$, $p_A = 0.96$	0.2829 ± 0.0004	0.284
$\kappa = 1/3$, $p_A = 1.00$	0.3087 ± 0.0005	0.306
$\kappa = 3$, $p_A = 0.96$	0.6872 ± 0.0004	0.697
$\kappa = 3$, $p_A = 1.00$	0.7017 ± 0.0003	0.713

data for different p_A collapse onto a single master curve, indicating that the loop statistics do indeed obey eq 10 (equally good collapse was found for $\kappa = 3$ and $1/3$). The slope of the plot gives the exponent α in eq 10. Note that the data points from high molecular weight bins are very noisy as there are only a few molecules in these bins. In order to reduce the impact of these data points on the fitting, we weighted each data point according to the number of molecules in that bin when performing the least-squares fit. This procedure yielded the fitting parameters $\alpha = 3.05 \pm 0.03$ for $\kappa = 1$, $\alpha = 2.94 \pm 0.01$ for $\kappa = 1/3$, and $\alpha = 3.13 \pm 0.09$ for $\kappa = 3$, indicating that α is universal with respect to κ to a good approximation. This value of α is higher than the value $\alpha = 2.5$ found by Jacobson and Stockmayer[31] for linear systems and indicates that there are fewer large loops in the HBP system. This is reasonable since looping is more likely in our system due to the large number of terminal groups.

In Table 3, we report values of DB from our simulation for different values of p_A and κ compared to the mean-field predictions of Holter and Frey.[14] We see that there is excellent agreement between simulation and theory across all values of p_A and κ. In particular, both simulation and theory show that increasing κ leads to a significant increase in DB, which is what one would expect. The close agreement between simulation and mean-field theory indicates that while fluctuations have a significant influence on the large-scale structure of HBPs (τ, d_f, etc.), its effect on the local structure of HBPs is much smaller. This is reasonable since fluctuation effects such as loop formation are generally larger scale phenomenon. We therefore do not expect these to have a significant influence on local reaction statistics.

5. Conclusion

We have studied the branching statistics of hyperbranched polymers formed from a one-pot melt polymerization of AB_2 monomers via Monte Carlo simulation of a percolation-type lattice model. Specifically, the molecular weight distribution, fractal structure, loop statistics, and degree of branching were studied as a function of both the fraction of reacted A groups p_A and the reactivity ratio κ.

For $p_A \rightarrow 1$, we found that the number density $n(N)$ of hyperbranched polymers with different p_A and κ collapse remarkably well onto a universal curve of the form $n(N)N_w^2 = A(N/N_w)^{-\tau} \exp(-BN/N_w)$, where A, B, and τ are independent of p_A and κ. From fitting the universal curve, we find $\tau = 1.32 \pm 0.01$, which is significantly different from the mean-field value of $\tau = 1.5$ and demonstrates the importance of fluctuations in our system. An alternative method for determining τ based on scaling N_w vs N_n gave values of τ which varied significantly with κ. This variation is inconsistent with our universal curve analysis which shows that τ is universal with respect to variations in κ. We attribute this variation to the fact that the characteristic mass of our HBP system N_{char} is not very large so that N_n is very sensitive to the lower cutoff mass. This introduces significant systematic errors into the analysis which makes the values of τ determined from the N_w vs N_n scaling unreliable. We therefore conclude that direct fitting of the universal curve explicitly including the cutoff function represents the most accurate means for determining τ for HBP systems. Finally, we have analyzed our number density data by fitting the apparent linear region as per the simulation study of Cameron et al.[8,9] and the experimental study of Kunamaneni et al.[26,27] We find values of τ which are consistent with these studies ($\tau \approx 1.5$). We emphasize, however, that these values are probably in error due to the neglect of the effect of the cutoff function.

For the fractal dimension d_f of HBP chains in the reaction melt, our results from scaling R_{gi} vs N_i and R_{gz} vs N_w, N_z yield results that are within error either the same or very close to the hyperscaling prediction of Buzza[24] ($d_f = 3$). Our results are significantly different from the mean-field result of $d_f = 4$, which again shows the importance of fluctuation effects such as looping and excluded volume interactions. They are also different from the percolation result of $d_f = 2.53$, thus confirming the fact that HBPs do not belong to the same universality class as randomly branched polymers in the percolation class.

For the loop statistics, we find that the number density of loops with degree of polymerization m obeys the scaling form $\hat{R}_m \propto m^{-\alpha} p_A^m$, with $\alpha \approx 3$ for all κ. This is higher than the value $\alpha = 2.5$ found by Jacobson and Stockmayer[31] for linear systems, which indicates that looping is more likely in our HBP system due to the large number of terminal groups compared to linear systems. Finally, for the degree of branching, we find excellent agreement between our simulations and the mean-field predictions of Holter and Frey.[14] We conclude from this fact that while fluctuations have a significant influence on the large-scale structure of HBPs (τ, d_f, etc.), its effect on the local structure of HBPs is much smaller.

The agreement between our results and experiments and higher resolution simulation data (when the data are analyzed in a consistent way) indicates that our minimal model captures the essential physics of real systems and is thus a useful tool

for constructing realistic HBP structures for further molecular simulations.

References and Notes

(1) Flory, P. J. *J. Am. Chem. Soc.* **1952**, *74*, 2718.
(2) Flory, P. J. *Principles of Polymer Chemistry*; Cornell University Press: Ithaca, NY, 1953.
(3) Hobson, L. J.; Feast, W. J. *Chem. Commun.* **1997**, *21*, 2067.
(4) Widmann, A. H.; Davies, G. R. *Comput. Theor. Polym. Sci.* **1998**, *8*, 191−199.
(5) Lyulin, A. V.; Adolf, D. B.; Davies, G. R. *Macromolecules* **2001**, *34*, 3783.
(6) Sheridan, P. F.; Adolf, D. B.; Lyulin, A. V.; Neelov, I.; Davies, G. R. *J. Chem. Phys.* **2002**, *117*, 7802.
(7) Galina, H.; Lechowicz, J. B.; Potoczek, M. *Macromol. Symp.* **2003**, *200*, 169−179.
(8) Cameron, C.; Fawcett, A. H.; Hetherington, C. R.; Mee, R. A. W.; McBride, F. V. *J. Chem. Phys.* **1998**, *108*, 8235.
(9) Cameron, C.; Fawcett, A. H.; Hetherington, C. R.; Mee, R. A. W.; McBride, F. V. *Macromolecules* **2000**, *33*, 6551.
(10) Beginn, Y.; Drohmann, C.; Moller, M. *Macromolecules* **1997**, *30*, 4112−4116.
(11) Muller, A. H. E.; Yan, D.; Wulkow, M. *Macromolecules* **1997**, *30*, 7015−7023.
(12) Yan, D.; Muller, A. H. E.; Matyjaszewski, K. *Macromolecules* **1997**, *30*, 7024−7033.
(13) Holter, D.; Burgath, A.; Frey, H. *Acta Polym.* **1997**, *48*, 30.
(14) Holter, D.; Frey, H. *Acta Polym.* **1997**, *48*, 298−309.
(15) Radke, W.; Litvinienko, G.; Muller, A. H. E. *Macromolecules* **1998**, *31*, 239−248.
(16) Hanselmann, R.; Holter, D.; Frey, H. *Macromolecules* **1998**, *31*, 3790−3801.
(17) Yan, D.; Zhou, Z.; Muller, A. H. E. *Macromolecules* **1999**, *32*, 245−250.
(18) Yan, D.; Zhou, Z. *Macromolecules* **1999**, *32*, 819−824.
(19) Schmaljohann, D.; Barrat, J. G.; Komber, H.; Voit, B. I. *Macromolecules* **2000**, *33*, 6284−6294.
(20) Zhou, Z.; Yan, D. *Polymer* **2000**, *41*, 4549−4558.
(21) Galina, H.; Lechowicz, J. B.; Walczak, M. *Macromolecules* **2002**, *35*, 3253.
(22) de Gennes, P. G. *J. Phys. (Paris)* **1977**, *38*, L355−L358.
(23) deGennes, P. G. *Scaling Concepts in Polymer Physics*; Cornell University Press: Ithaca, NY, 1979.
(24) Buzza, D. M. A. *Eur. Phys. J. E* **2004**, *13*, 79−86.
(25) Colby, R. H.; Rubinstein, M. *Polymer Physics*; Oxford University Press: New York, 2003.
(26) Suneel; Buzza, D. M. A.; McLeish, T. C. B.; Parker, D.; Keeney, A. J.; Feast, W. J. *Macromolecules* **2002**, *35*, 9605.
(27) Kunamaneni, S.; Buzza, D. M. A.; Parker, D.; Feast, W. J. *J. Mater. Chem.* **2003**, *13*, 2749.
(28) Note that our definition of τ and the cutoff function in eq 2 is different from that used in eqs 6.118 and 6.122 in ref 25. In the latter two equations, the number density for HBPs is written as $n(N) = N^{-2}(N/N_{char})^{2-\tau} f(N/N_{char}) = N^{-\tau_F} \tilde{f}(N/N_{char})$, where $\tau_F = 2$ is the Fisher exponent and $\tilde{f}(N/N_{char}) = (N/N_{char})^{2-\tau} f(N/N_{char})$ is a modified cutoff function which contains a power law in N/N_{char}. The two forms for $n(N)$ are obviously equivalent. In this paper, we choose to work with the form given by eq 2 since we prefer to work with a cutoff function that has no hidden power law scaling.
(29) Stauffer, D.; Aharony, A. *Introduction to Percolation Theory*, revised 2nd ed.; CRC Press: London, 1994.
(30) Cates, M. E. *J. Phys., Lett.* **1985**, *46*, L837−L843.
(31) Jacobson, H.; Stockmayer, W. H. *J. Chem. Phys.* **1950**, *18*, 12.
(32) Richards, E. L. Monte-Carlo Studies of Hyperbranched Polymerization. M. Res. thesis, Leeds University, 2006.
(33) Lusignan, C. P.; Mourey, T. H.; Wilson, J. C.; Colby, R. H. *Phys. Rev. E* **1995**, *52*, 6271.
(34) Lusignan, C. P.; Mourey, T. H.; Wilson, J. C.; Colby, R. H. *Phys. Rev. E* **1999**, *60*, 5657.

MA0700126